ELSEVIER

Polymer 41 (2000) 3193–3203

polymer

Processing and characterization of reactive polystyrene/hyperbranched polyester blends

T.J. Mulkern*, N.C. Beck Tan

US Army Research Laboratory, Weapons and Materials Research Directorate, Weapons Materials Research Division—Polymers Research Branch, Aberdeen Proving Grounds, MD 21005-5069 USA

Received 5 March 1999; accepted 28 July 1999

Abstract

Newly developed hyperbranched polyols (HBPs) possess a compact, highly branched, three-dimensional (3D) structure, which has a high density of functional end groups and inherently low viscosity. The combination of these two properties, low viscosity and high reactivity, makes HBP polymers attractive candidates for reactive polymer blending. The HBP additives are able to behave as lubricants during processing and as self-compatibilizing toughening agents in the final blend formulation. In this work, we have studied a series of blends of hyperbranched polyester with high molecular weight polystyrenes. The processability and compatibility in the blends were investigated as a function of volume fraction of the HBP added and reactivity of the matrix phase. We find, through processing and rheological studies, that HBPs are extremely effective processing aids. A significant drop in the blend viscosity occurs immediately on addition of HBP, even at levels as low as 2 vol.%. Characterization including microscopy, thermal analysis and Fourier transform infrared spectroscopy (FTIR) indicates that the HBP forms immiscible blends with polystyrene and styrene maleic anhydride (SMA) copolymers. A significant degree of compatibilization occurs in the reactive systems, as evidenced by shifts in the thermal transitions of the HBP phase, and by morphology refinement observed by electron microscopy. The degree of compatibilization in the blends was found to increase with SMA reactivity.

Keywords: Reactive blends; Hyperbranched polymer; Dendrimer

1. Introduction

Dendritic polymers are a new class of three-dimensional (3D), man-made molecules produced by an unusual synthetic route that incorporates repetitive branching sequences to create an unusual architecture. Over the last few years, dozens of patents have been filed on the synthesis of dendritic polymers of varying chemistries [1–12]. Applications for this technology are being proposed in fields as diverse as gene therapy and commercial coatings [13–32]; however, actual exploitation of dendritic polymer technology is still in its infancy, largely due to the limited availability of these new materials and the expense of their synthesis.

Recently, dendritic polymers have been produced by a new, lower cost hybrid synthetic process that generates ultrabranched, polydisperse molecules. These materials are called hyperbranched polymers to distinguish them from their more perfect, monodisperse cousins, 'dendrimers' and are being produced in sufficient quantities to allow for investigation of their utility in conventional engineering applications (Fig. 1). Unique features of the dendritic architecture which make them attractive for many applications result directly from the repetitive branching which occurs during their synthesis and include a very compact structure and an extremely high density of functional, terminal groups. Due to the compact, 3D structure of dendritic polymers these molecules mimic the hydrodynamic volume of spheres in solution or in the melt and flow easily past each other under applied stress. This results in a low melt viscosity, even at extremely high molecular weights, due to a lack of restrictive inter-chain entanglements [33]. In fact, dendritic polymers have been shown to exhibit melt and solution viscosities that are an order of magnitude lower than linear analogues of similar molecular weight [34–37]. The high density of functional terminal groups on dendritic polymers also offers the potential for tailoring their compatibility with other polymers, either through conversion of dendritic polymer endgroups to chemically suitable moieties or through in situ reaction to form covalently bound networks or dendritic copolymer compatibilizers. These two properties of dendritic polymers, low viscosity and tailorable compatibility, make them

* Corresponding author. Tel.: +1-410-306-0692; fax: +1-410-306-0676.

0032-3861/00/$ - see front matter
PII: S0032-3861(99)00543-1

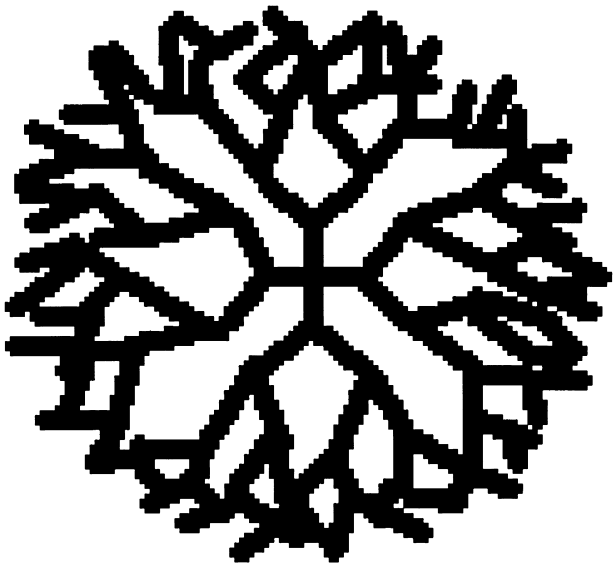

Fig. 1. Schematic illustration of hyperbranched polymer architecture.

excellent candidates for additives that could act simultaneously as processing aids and toughening agents. In fact, dendritic polymers have been successfully employed to improve both processability and toughness in thermoset resins through a controlled reactive phase separation process [38,39].

To date, studies on dendritic polymer/thermoplastic blends have been limited to miscible and/or unreactive systems [37,40]. These studies have demonstrated the promise of dendritic polymers for use as rheology modifiers and processing aids. However, no studies have been aimed directly at assessing the use of dendritic polymers as components in a polymer blend with controlled morphology designed to enhance mechanical performance. The abundance of functional terminal groups on these molecules makes them good candidates for reactively compatibilized blends, in which co-reactive moieties on the dendritic polymer and matrix polymer would form compatibilizers in situ during processing. These compatibilizers act to lower the interfacial tension in a multiphase blend, to increase the interfacial adhesion, and to stabilize the dispersion against coarsening during processing or subsequent forming operations, and generally enhance blend performance [41–43]. In addition, the benefit of low melt viscosity in the dendritic polymers may counterbalance the increase in viscosity that is often encountered during reactive blending as a result of copolymer formation and the associated molecular weight buildup [44–46]. Thus, the combination of low melt viscosity and high reactivity may make dendritic polymers an ideal choice for thermoplastic blend modifiers which can enhance both properties and processability.

It is the aim of this work to investigate the incorporation of dendritic polymers into a reactive, immiscible, thermoplastic blend system. Issues addressed are the identification of proper processing techniques for blending of these low viscosity additives into a high molecular weight thermoplastic matrix, assessment of any benefits in processability resulting from the addition of dendritic polymers, and evaluation of the extent of compatibilization achieved in such a highly reactive system.

2. Experimental details

2.1. Materials

A nonreactive polystyrene (PS) and two reactive styrene maleic anhydride (SMA) resins with different maleic

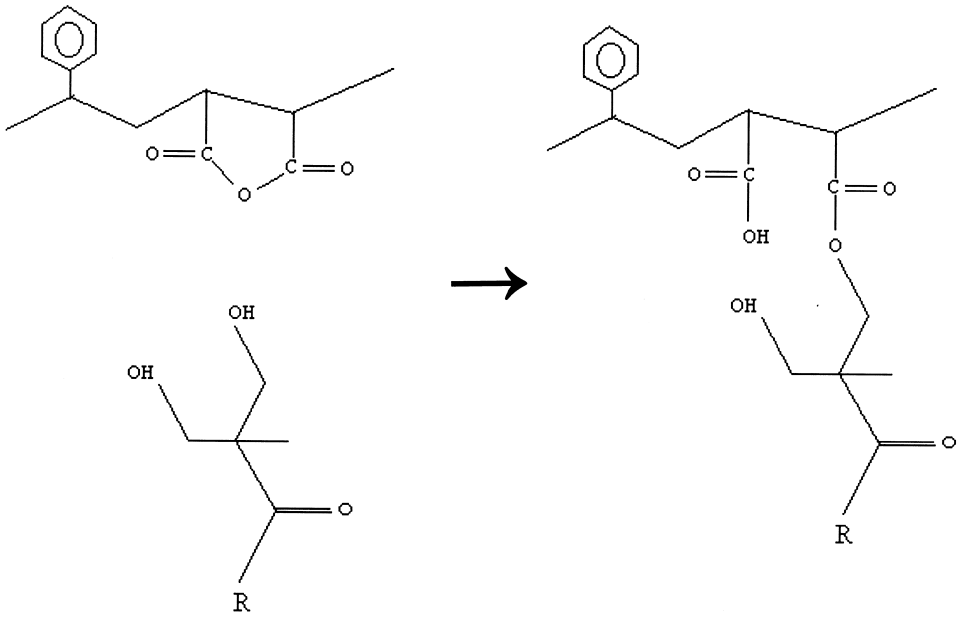

Fig. 2. Expected reaction between styrene maleic anhydride and hyperbranched polyol.

Table 1
Estimated ratio of reactive groups in blends

Matrix	HBP (wt%)	MA/–OH
SMA9	2.00	5.27
SMA9	5.00	1.96
SMA9	10.00	0.96
SMA14	2.00	7.92
SMA14	5.00	2.94
SMA14	10.00	1.45
PS	2.00	0.00
PS	5.00	0.00
PS	10.00	0.00

anhydride (MA) content were chosen for melt blending with a hyperbranched polyol (HBP) having hydroxyl-terminated end groups.

The dendritic polymers chosen are fourth-generation (G4) Perstorp Hyperbranched Polyols. These are developmental materials based on polyester chemistry and have, on average, 64 –OH terminated end groups per molecule, and theoretical molecular weight and polydispersity index of 7300 g/mol and 2.0, respectively. The HBP molecules are synthesized from a Pentaerythritol ($C_5H_{12}O_4$) core and multiple 2,2-dimethylol propionic acid ($C_5H_{10}O_4$) chain extenders or repeat units. These developmental resins were supplied in small quantities with little technical data and are now commercially available in moderate quantities under the trade name of Boltorn [47].

The two types of SMA random copolymer used were produced by ARCO and marketed under the trade names Dylark 232 and Dylark 332 [48]. Both materials are general purpose transparent grade resins. Molecular weights and polydispersity indexes were reported by the manufacturer to be 200 000 g/mol and 2.0, respectively, for Dylark 232, and 180 000 g/mol and 2.0, respectively, for Dylark 332. Elemental analysis showed that Dylark 232, designated SMA9, contained 9.11% MA by weight and that Dylark 332, designated SMA14, contained 13.9% MA by weight. The PS resin used is a general purpose grade transparent resin, manufactured by Dow Chemical under the trade name Styron 685D [49], with molecular weight of 300 000 g/mol and polydispersity index 2.6, as reported by the manufacturer.

SMA copolymers are frequently used in reactively compatibilized blend systems due to the reactivity of the MA with various functional groups [43,50–54]. In the co-reactive system studied here, a ring opening reaction takes place between the SMA and the –OH functional groups on the HBP, generating an acid and an ester functionality (Fig. 2). Covalent bonds are thus formed between the two polymer molecules generating copolymer compatibilizers.

2.2. Blends

Nine polymer blends and three controls were prepared. PS, SMA9 and SMA14 materials were each blended with 0, 2, 5 and 10% HBP by weight. The 10% blends were fully characterized. The highest concentration of HBP that could be blended was 10% by weight due to the mismatch in viscosity between the matrix material and the HBP polymers as well as the limitations of the processing equipment.

For each of the blends prepared, the number of functional groups on the PS, SMA and HBP for a given mass of polymer along with the ratio of reactive groups present was estimated (Table 1). In all reactive blends there was an excess of MA functional groups relative to HBP hydroxyl functional groups, except for the SMA14/10% HBP blend where the ratio was nearly unity.

The blends were mixed in small batches of approximately 65 g in the Haake Rheomix 600 mixer driven by a Haake Rheocord 40 System. All of the blends were processed under the same conditions. The processing temperature for the blends was 200°C, which is on the lower end of the processing window for both the PS and SMA materials. This temperature was selected due to the thermal instability of the HBP above 200°C, as determined by thermogravimetric analysis (TGA) [55]. The blends were prepared by first melting the PS or SMA in the mixer followed by the addition of the HBP. Once the HBP was added to the molten base polymer, the two materials were blended for 15 min to ensure a proper degree of mixing and sufficient time for reaction. The processing speed was 55 rpm, which corresponds to a shear rate in the range of 42–63 s^{-1} [56].

Solution blends for Fourier transform infrared spectroscopy (FTIR) studies were prepared by dissolving equal weights of SMA and HBP in THF at 50°C. The polymer blend was recovered by precipitation into water, a non-solvent for both polymer species. The blend precipitate was dried and annealed at 200°C for 30 min to allow reaction under simulated processing conditions.

2.3. Characterization

2.3.1. Rheology

Post-processing rheological studies were carried out according to ASTM Standard D4440-95. A Rheometrics System 4 parallel plate rheometer was used in a frequency sweep mode over a range of 0.01–100 s^{-1} at 10% strain. The testing temperature of 200°C was used for measurement to simulate processing conditions.

2.3.2. Morphology

Morphology was evaluated using scanning electron microscopy. Samples were prepared by freezing the polymer blends in liquid nitrogen followed by high-speed impact to create fresh fracture surfaces. To improve contrast for image analysis, the dispersed phase was removed by submerging the samples in methanol, a selective solvent for the HBP. Fracture surfaces were examined with an Electroscan 2020 Environmental Scanning Electron Microscope. Image analysis techniques were employed in

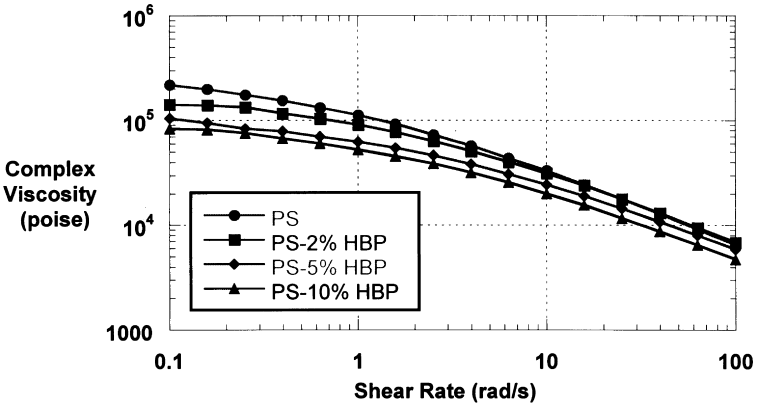

Fig. 3. Rheological behavior of PS with the addition of HBP.

order to determine the average particle size and size distribution.

2.3.3. Thermal analysis

Glass transition temperatures for the pure polymers and the 10% HBP blends were evaluated using a TA Instruments DSC 2920. Samples were scanned twice at a rate of 20°C/min over a temperature range from −40°C to 200°C. The DSC cell was purged with ultra high purity nitrogen gas at a constant flow rate of 80 cc/min to prevent sample degradation.

2.3.4. FTIR

FTIR studies were performed on all pure polymers and blends on a Perkin–Elmer Spectrum 2000 FTIR Spectrometer. The samples were prepared by first dissolving the polymer blend in THF, applying a few drops of the solution onto a 25 × 4 mm potassium bromide crystal and drying in a vacuum oven at 50°C for 10 min. Data from an average of 16 scans over a range of 4000–400 cm^{-1} at a resolution of 2 cm^{-1} were analyzed using Perkin–Elmer Spectrum v2.0 software.

3. Results and discussion

3.1. Processing characteristics

The blending of PS and SMA with the HBP was challenging due to the small quantity of the HBP available as well as the melt characteristics of the HBP. The HBP has an extremely low melt viscosity compared to that of the PS or SMA and tended to remain segregated in the melt unless an aggressive mixing scheme was implemented.

Due to the small amount of HBP available for study the first attempt at blending was in a low capacity experimental CSI Max Mixing extruder. This process was aborted due to poor mixing efficiency, short residence time and an extremely low output of the instrument.

The second attempt at blending with a Haake Polylab System fitted with a single screw extruder was an improvement due to the higher output of material and precise monitoring of processing parameters. It was observed that with as little as 2% HBP by weight added, the torque and pressure in the extruder dropped an order of magnitude relative to the torque required to process the pure PS or SMA under the same conditions. This indicates a significant reduction in the processability of the blend due to the addition of HBP, and is believed to be the result of the lubrication of the extruder barrel wall. This is due to the migration of the HBP molecules to the surface. Khadir and Gauthier observed a similar effect in their studies of linear/hyperbranched PS blends [37]. Although an improvement over the low-capacity CSI mixer, the mixing efficiency and residence time provided by the single screw extruder was not sufficient to provide good blending. The HBP tended to lag behind in the extruder barrel and a variation in the degree of mixing was apparent upon inspection of the extrudate. In order for these materials to blend efficiently it was obvious that a more aggressive mixing process had to be implemented.

Ultimately, the blends were mixed in small batches in a Haake counter rotating blade mixer. This system provides aggressive batch mixing conditions, allowing sufficient time for the material to melt, mechanically break up and mix. Unfortunately, online monitoring of torque/pressure inside the mixer was not available, hence post-processing rheological studies were conducted in order to assess 'processability' of blends relative to pure materials.

The rheological properties of all the blends were found to change dramatically with the addition of HBP. In all cases, blend viscosity was lower than the viscosity of the pure matrix material (PS or SMA), indicating that an improvement in processability results from the incorporation of HBP. In the PS/HBP system, the viscosity dropped with the addition of as little as 2% HBP by weight and continued to drop as more HBP was added (Fig. 3). In the reactive SMA/HBP blends the viscosity also dropped significantly with the initial addition of 2% HBP. Further addition of HBP produced successively lesser reductions in melt viscosity in these systems (Fig. 4).

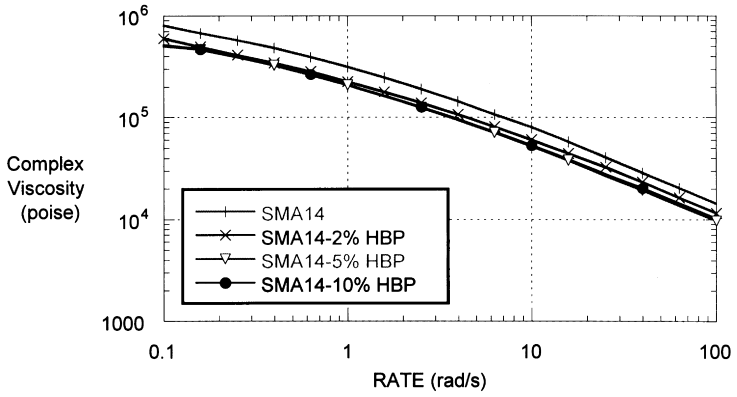

Fig. 4. Rheological behavior of SMA14 with the addition of HBP.

The rheological data at a constant shear rate are plotted in Fig. 5 to underscore the difference in behavior exhibited by the reactive and non-reactive blends. The continuous drop in viscosity of the PS/HBP blend seems to be an additive effect, which correlates with the amount of HBP present. The viscosity of the SMA/HBP blend is stabilized at higher HBP content after the initial drop. This may be the result of competing mechanisms taking place in the reactive blends. The HBP acts as a processing aide because of its molecular structure and low molecular weight, decreasing the melt viscosity. At the same time, crosslinking and/or molecular weight buildup associated with the compatibilization reaction is occurring in the blends. As more HBP is added, the propensity for reaction should increase, counterbalancing the lubrication effect of the HBP.

The rheological behavior observed for the SMA/HBP blends is not consistent with most reactive blending schemes whereby there is typically a significant increase in the viscosity or torque as compatibilization reactions take place [46]. A lowered viscosity is, however, consistent with the melt viscosity behavior of hyperbranched molecules and is attributed to the compact molecular structure of the HBP [37]. In addition, the HBP–SMA copolymer compatibilizers which result from the reaction have a linear/hyperbranched hybrid architecture, which is also compact relative to linear architectures of equivalent molecular weight, and has a reduced tendency for chain entanglement promoting a lower viscosity [35].

3.2. Morphology

The morphology observed from the fracture surfaces of the PS/HBP and the SMA/HBP blends are consistent with expectations based on past research in the area of reactive polymer blends [50]. The PS/10% HBP blend exhibits a coarse microstructure with large second-phase particles that is characteristic of an immiscible blend. The average particle size in the PS/HBP blend is 7.70 μm in diameter (Fig. 6, Table 2). Large HBP particles remain phase separated in a PS matrix at equilibrium due to the lack of compatibility in the system. Coalescence of the HBP phase may also be taking place as the blend cools after processing. This type of morphology is not likely to improve the mechanical properties of the PS homopolymer due to the large particle size and lack of compatibilization at the polymer/polymer interface [57–59].

The morphology of the reactive blends (Figs. 7 and 8) show a smaller average particle size relative to the PS/HBP

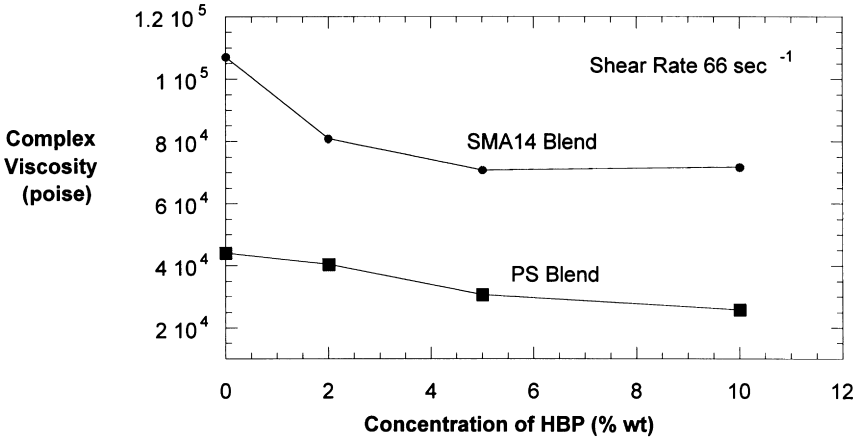

Fig. 5. Change in viscosity at constant shear rate of 66 s^{-1} (chosen to approximate blending conditions, see Section 2).

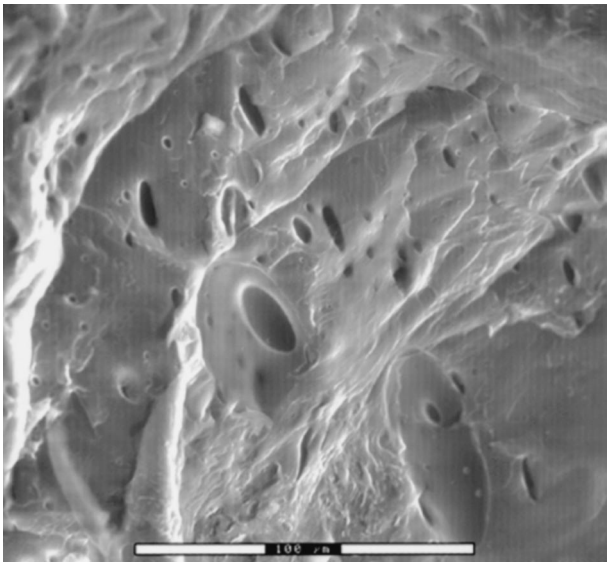

Fig. 6. PS/10% HBP blend fracture surface.

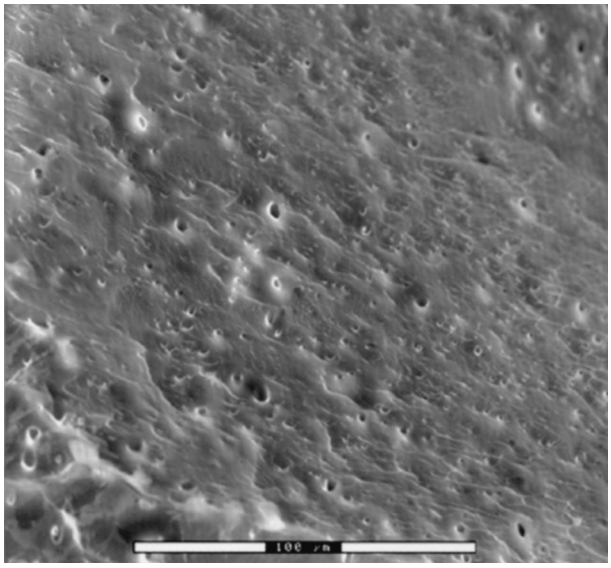

Fig. 7. SMA9/10% HBP blend fracture surface.

blend. This observed decrease in particle size in the SMA blends may be attributed to a reduction of the interfacial tension and to a restriction of particle coalescence during processing which results from the formation of a copolymer compatibilizers [60–62]. The average particle size in both the SMA9/10% HBP and the SMA14/10% HBP blends is approximately 1 μm (Figs. 7 and 8, Table 2). No significant refinement in morphology was observed with increase in MA content from 9 to 14%, indicating that 9% or less is sufficient for compatibilization in this system.

Though there is clearly a difference between the second-phase particle size between the PS blends and the SMA blends, the observed differences cannot be attributed solely to the effects of compatibilization, given the differences in viscoelastic properties of the styrenic matrix materials. In order to gauge the importance of these effects, second-phase particle sizes may be estimated based solely on properties of the PS, SMA9 and SMA14 matrices, for comparison with the particle sizes observed in the blends.

According to Taylor [63], the size of the second-phase particles in an immiscible, two-phase system can be estimated from the following equation:

$$d = (\gamma_{AB}/G\eta_m)/(16\lambda + 16/19\lambda + 16) \quad (1)$$

where d is the particle diameter, γ_{AB} the interfacial tension between the components, G the shear rate and λ the ratio between the dispersed phase viscosity and the matrix phase viscosity, η_d/η_m. This theory was originally developed for Newtonian droplets dispersed in a Newtonian fluid under steady shear flow and therefore, cannot be strictly applied to polymer melts. However, it is considered to be an acceptable starting point for most modern work on droplet dispersion and coalescence, suitable for initial predictions [64,65]. For these calculations, HBP viscosity was estimated from information supplied by the manufacturer [66], viscosities measured at 200°C and 66 s^{-1} were used for SMA resins (see Sections 2 and 3.1), and interfacial tension was assumed to be constant. Particle size predictions are presented in the form of d_{blend}/d_{PS} blend, due to lack of a suitable estimate for the interfacial tension.

Table 2
10% HBP blends; second-phase particle size distribution

	SMA1	SMA2	PS
Average diameter ($m \times 10^{-6}$)	1.1	1.0	7.7
Standard deviation ($m \times 10^{-6}$)	0.7	0.4	5.3
Population	50.0	74.0	70.0
95% confidence interval	0.2	0.1	1.3

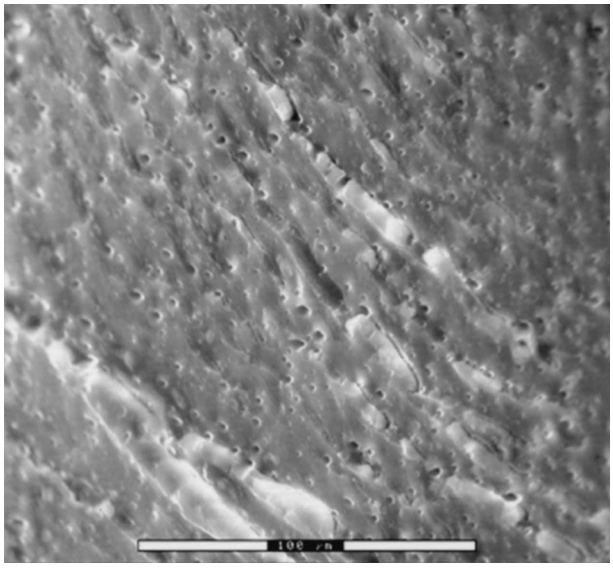

Fig. 8. SMA14/10% HBP blend fracture surface.

Table 3
Taylor predictions of relative size of second-phase particles

	G (s^{-1})	h_m (P)	h_d (P)	l	d/γ_{AB}	d_{blend}/d_{PS}
PS	66	9200	600	0.650	1.63×10^{-6}	1.00
SMA9	66	10700	600	0.560	1.4×10^{-6}	0.86
SMA14	66	30390	600	0.029	7.39×10^{-7}	0.45

Based on the predictions from Eq. (1), a difference in particle size should be expected for PS, SMA9 and SMA14 matrix blends as a result of differences in matrix melt viscosity (Table 3). The minor phase particles in the SMA9 and SMA14 blends are predicted to be 85 and 45%, respectively, of the size of the minor phase particles in the PS blend. These calculations correctly predict that the particle size in the reactive systems should be smaller than in the unreactive blends. However, the magnitude of the dispersed phase size reduction observed is much larger than predicted from these simple dispersion arguments, and the particle size analysis showed no significant difference between particle sizes in the SMA9 and SMA14 blends. Therefore, the observed morphology refinements in the SMA/HBP blends cannot be attributed solely to viscoelastic effects, and successful reactive compatibilization is most likely making a significant contribution to the observed morphology refinement. This type of morphology refinement is indicative of the formation of copolymers through the reaction of SMA and HBP, which has been confirmed independently via spectroscopy and thermal analysis.

3.3. Thermal transitions

It is well established that shifts in the glass transition temperature (T_g) of component polymers can be used to evaluate miscibility and immiscibility in polymer blends [67,68]. DSC was performed on all of the individual polymers and the 10% HBP polymer blends to determine pure component T_gs and any subsequent shifts after blending as a result of compatibilization. All of the blends under study exhibited two distinct T_gs, each of which is associated with an individual blend component (Figs. 9 and 10, Table 4). The presence of the two distinct T_gs coupled with the microscopy investigation confirms blend immiscibility.

The thermal analysis results for the PS/HBP blend showed behavior typical of an immiscible, uncompatibilized blend in which no significant deviations from the pure component values were observed for either T_g exhibited by the blend. Thermal analysis results from reactive blends confirm some degree of compatibilization. The T_g associated with the SMA component did not shift significantly from that of the pure matrix value in any SMA/HBP blend. However, the T_g associated with the HBP component in the HBP/SMA blends exhibited a positive shift towards the T_g of the SMA component. A positive shift of the second-phase T_g is an indication of reaction and the incorporation of SMA in the HBP phase. In both 10% reactive blends, the results indicated that the second-phase is an intimate mixture of HBP and SMA while the matrix phase remains essentially pure SMA.

The size of the $T_{g,HBP}$ shift observed increased with an increase in the MA concentration in the SMA matrix (Table 4). The SMA9/HBP blend exhibited a moderate T_g shift of about 5.2°C. The more reactive SMA14 blend exhibited a larger T_g shift of 9.6°C. As mentioned previously, this increase in the T_g of the HBP phase is indicative of the incorporation of SMA molecules into this phase. Both the quantity and the T_g of the pure SMA copolymer being incorporated dictate the size of the shift in T_g. If the dispersed phase is considered to be an intimate mixture of SMA and HBP, i.e. a miscible blend, a simple analysis may be performed to estimate its composition.

In a miscible blend, a single T_g is typically observed in between the T_gs of the individual components [69]. The position of the blend T_g ($T_{g,b}$) is related to the mass fraction (m_i) and $T_{g,i}$ of the individual components, $i = 1, 2$, by the

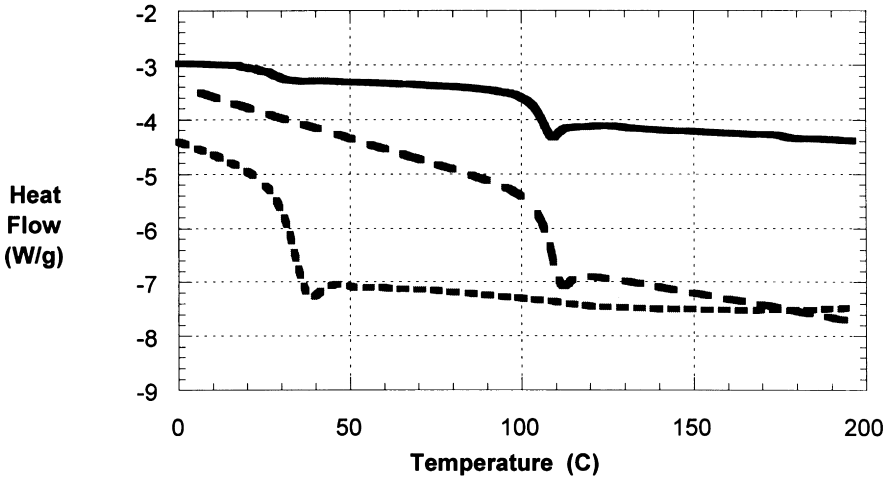

Fig. 9. DSC curves: PS blend (top), PS (middle) and HBP (bottom).

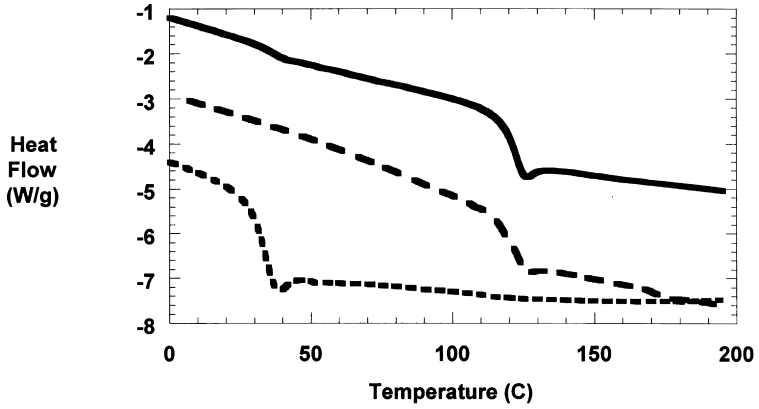

Fig. 10. DSC curves: SMA9 blend (top), SMA9 (middle) and HBP (bottom).

Fox equation [70]:

$$1/T_{g,b} = m_1/T_{g,1} + m_2/T_{g,2} \quad (2)$$

Coupling equation (2) with the mass balance, $m_1 + m_2 = 1$, and the measured T_g values allows one to solve for the mass fractions, m_{HBP}, m_{SMA}, of the individual polymers in the dispersed phase. The calculations estimate the incorporation of ~6% SMA9, by weight, in the minor phase of the SMA9/10% HBP blend, and the incorporation of ~11% SMA14, by weight, into the dispersed phase of the SMA14/10% HBP blend (Table 5).

This increase in the percentage of SMA incorporated into the HBP phase as a function of MA content in the matrix implies an increase in compatibility as a function of increased matrix reactivity. As the compatibility between the two phases increases, an improvement in mechanical properties may result due to improved interfacial adhesion. However, in cases in which mechanical toughening is desired (a common reason for blending) the larger increase in T_g associated with the more reactive system may be detrimental, particularly if not accompanied by the benefit of additional morphology refinement as is the case in the SMA/HBP system.

3.4. Confirmation of reaction

FTIR spectroscopy was used in order to confirm the reaction in SMA/HBP blends. Scans of the pure materials were taken before blending in order to obtain a baseline. FTIR spectra were taken for the SMA/10% HBP blends, and the peaks characteristic of the MA ring were scrutinized. The results suggested reaction but the data fell within the error of the spectrometer and were thus inconclusive. This is a consequence of the fact that while many reactions may take place during compatibilization, the total fraction of all MA rings in the system that react is very small. In fact, even if all MA species on the SMA chains that had been incorporated into the minor phase of the SMA14/10% HBP blend (see above) had reacted, only ~1% of the total number of MA rings present in that blend would have been affected. Unfortunately, no other signature absorptions occur in the system that are suitable for quantitative analysis of reaction in the melt processed blends (Fig. 2).

For completeness, to confirm that the SMA and HBP materials react under the thermal conditions employed during blending, model solution blends were prepared and heat treated under simulated processing temperatures. These model blends contained 50% HBP, or a 9:1 ratio of hydroxyl to MA functional groups to greatly increase the likelihood of the ring opening reactions occurring for all MA species present and therefore, increase the likelihood of detection.

The MA ring present in the SMA resins absorbs strongly at 1781 cm^{-1} (Fig. 11). This spectral region has been highlighted for the SMA14/HBP solution blend along with its pure components in Fig. 12. Clearly, the relative strength of the MA absorption (1781 cm^{-1}) to the SMA reference absorption (1493 cm^{-1}) is significantly less in the blend than in the pure SMA. The 1493 cm^{-1}/1781 cm^{-1} absorption ratio increased from 0.46 in the pure SMA14 to 1.31 in the SMA/HBP blend (after normalization and subtraction of the HBP contribution to the blend spectra). The decrease in the strength of the MA absorption (1781 cm^{-1}) and

Table 4
Glass transition temperatures of pure components and two-phase blends

Material	HBP T_g (°C)	PS T_g (°C)	SMA9 T_g (°C)	SMA14 T_g (°C)
Pure component	32.0	109.0	124.0	135.0
PS blend	31.1	112.2	×	×
SMA9 blend	37.2	×	122.5	×
SMA14 blend	41.6	×	×	136.3

Table 5
Mass fraction of SMA incorporated into the minor phase of reactive blends

Matrix	T_g HBP (K)	T_g SMA (K)	T_g HBP phase (K)	Mass fraction SMA	Mass fraction HBP
SMA9	305.00	396.00	310.50	0.06	0.94
SMA14	305.00	408.00	314.00	0.11	0.89

increase in the ratio confirms that ring opening reactions are taking place under the simulated blending conditions, as expected. It is this reaction that is responsible for the in situ formation of SMA/HBP copolymer compatibilizers during processing that results in refinement of the morphology in reactive blends, and which may be exploited in the design of blends with improved performance relative to the analogous unreactive blends.

4. Conclusion

Hyperbranched polymer molecules have a unique, highly branched 3D structure and high density of functional endgroups. These factors make these new polymers attractive for use in blends, where their characteristics have the potential to be exploited to enhance blend processability as well as to facilitate in situ compatibilization in immiscible systems.

In this study, it has been demonstrated that hyperbranched polymers may be used successfully to produce self compatibilized thermoplastic blends with enhanced processing characteristics. Mixing of HBPs into high molecular weight polymers was challenging due to mismatched viscosity, but was accomplished successfully through implementation of aggressive mixing processes. Preliminary indications of enhanced processability came in the form of torque reduction during processing. A more comprehensive assessment of processability was undertaken via post-processing rheological studies. These experiments showed that a significant decrease in the melt viscosity of high molecular weight PS and SMA occurred on blending with as little as 2% of HBP. However, the dependence of viscosity on HBP content was observed to be different for reactive and unreactive blends. In the unreactive system, viscosity dropped in proportion to the amount of HBP added, indicating that the HBP was acting as a lubricant. In the reactive blend, melt viscosity decreased with the addition of up to 5% HBP, after which the blend viscosity remained essentially constant. This stabilization of the blend viscosity is believed to be the result of competition between the lubrication effect of the HBP and molecular weight buildup during processing due to interchain reactions in the functionalized systems. Further evidence for interchain reaction was provided on assessment of compatibilization in the system, including morphology studies, thermal analysis and spectroscopy.

Morphology studies using scanning electron microscopy showed that a two-phase morphology was characteristic of all blends, with more or less spherical droplets of the minor phase dispersed in a continuous matrix phase. While both reactive and unreactive systems were found to be immiscible, there was a large difference between the second-phase particle size between the two systems. The unreactive blends exhibit a coarse morphology with an average second-phase particle size of 7.7 μm in diameter. The reactive blends have a more refined morphology, with the second-phase particles averaging ~1.0 μm in diameter, indicative of the self compatibilization occurring in these systems during processing. No significant reduction in the second-phase particle size resulted on increasing the reactivity of the SMA matrix from ~9% MA by weight to ~14% MA by weight. However, thermal analysis revealed a stronger shift in the dispersed phase T_g in the SMA14

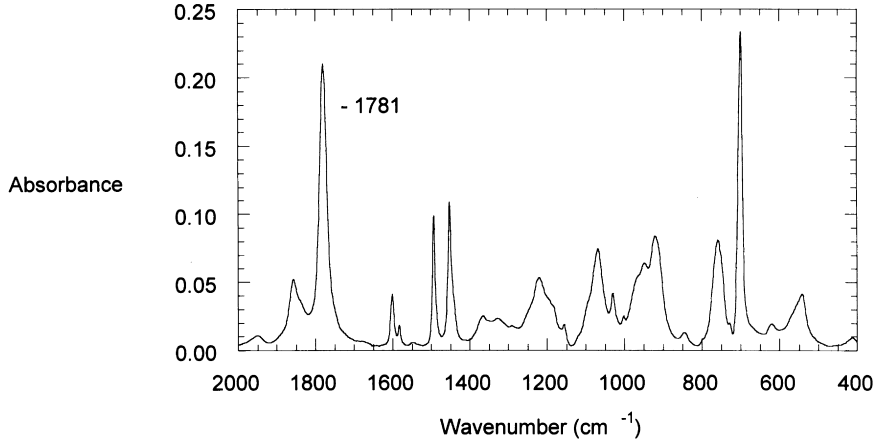

Fig. 11. FTIR spectra of styrene maleic anhydride 14.

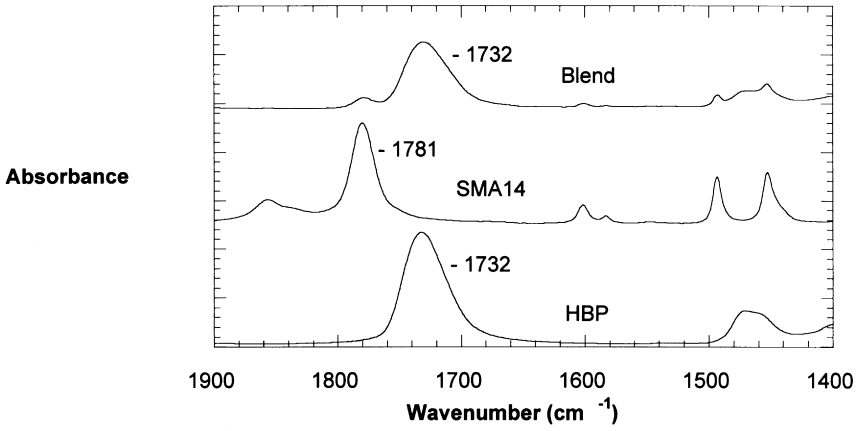

Fig. 12. FTIR spectra of SMA14 blend.

blend than in the SMA9 blend. Interpretation of this data revealed that the amount of SMA incorporated into the minor phase of compatibilized SMA/HBP blends increased significantly with matrix reactivity. The combined results of the morphology studies and thermal analysis indicate the occurrence of interchain reaction between hydroxyl functional groups on the HBP and the MA functionalities of the SMA to form copolymer compatibilizers. The occurrence of this ring opening reaction in the SMA/HBP system was confirmed by FTIR as well.

The combined results from processing, rheology, morphology and thermal analysis investigations of novel hyperbranched polymer blends indicate that these dendritic molecules may be incorporated successfully into thermoplastic blends. They offer the potential for design of blends with greater processability than conventional reactive systems, and a morphology that may be controlled via dendritic polymer end group reactions for optimization of blend performance.

Acknowledgements

We would like to thank the following for their efforts in this research: Mr Jeff Jones and Perstorp Polyols for their generous donation of experimental materials, Mr Donovan Harris of the US Army Research Laboratory for assistance with SEM studies, and Dr Steven Grossman and Prof. Stephen Driscoll of the University of Massachusetts Lowell for overall guidance and mechanical testing.

References

[1] Tomalia DA. US Patent 5773527, 1998.
[2] Hedstrand DM. US Patent 5393797, 1997.
[3] Frechet JT. US Patent 5041516, 1997.
[4] Hedstrand DM. US Patent 5387617, 1998.
[5] Newkome GR. US Patent 5773551, 1998.
[6] Matyjaszewski K. US Patent 5763548, 1998.
[7] Mager M. US Patent 5679755, 1998.
[8] Juneau KN. US Patent 5777129, 1998.
[9] Newkome GR. US Patent 5422379, 1998.
[10] Swanson DR. US Patent 5705573, 1998.
[11] Turner SR. US Patent 5196502, 1998.
[12] Klee JE. US Patent 5760142, 1998.
[13] Wright DC. US Patent 5795582, 1997.
[14] Jansen JF. US Patent 5788989, 1997.
[15] Hansen HJ. US Patent 5635603, 1997.
[16] Urdea MS. US Patent 5594118, 1998.
[17] Virtanen J. US Patent 5718915, 1998.
[18] Tezon JG. US Patent 5736346, 1998.
[19] Platzek J. US Patent 56501364, 1998.
[20] Platzek J. US Patent 5759518, 1998.
[21] Keefer LK. US Patent 5676963, 1998.
[22] Szoka FC. US Patent 5661025, 1997.
[23] Keefer LK. US Patent 5650447, 1997.
[24] Keefer LK. US Patent 5405919, 1995.
[25] Tomalia DA. US Patent 5714166, 1998.
[26] Mead SB. US Patent 5596027, 1997.
[27] Winnik FM. US Patent 5256516, 1998.
[28] Breton MP. US Patent 5266106, 1998.
[29] Winnik FM. US Patent 5098475, 1998.
[30] Milco LA. US Patent 5731095, 1998.
[31] Bahary WS. US Patent 5658574, 1998.
[32] Gundlach KB. US Patent 5254159, 1997.
[33] Billmeyer FW. Textbook of polymer science, New York: Wiley, 1984.
[34] Massa D, Shriner KA. Macromolecules 1995;28:3214.
[35] Frechet JM, J MS. Pure Appl Chem A33 1996;10:1399–425.
[36] Uppuluri S, Kenneth SE, Tomalia DA, Dvornic P. Macromolecules 1998;31:4498.
[37] Khadir A, Gauthier M. ANTEC'97 Proceedings, 1997. p. 3732.
[38] Boogh L, Peterson B. SAMPE J 1997;33.
[39] Boogh L, Petersson B, Månson JAE. Procceedings of the EPS Conference. Lausanne, 1–6 June 1997. p. 39–40.
[40] Carr PL, Davies GR, Feast WJ, Stainton NM, Ward IM. Polymer 1996;37:2395–2401.
[41] Wu S. Polymer 1985;26:1855.
[42] Simmons A, Baker WE. Polym Commun 1990;31:20.
[43] Dharmarajan N, Datta S, Ver Strate G, Ban L. Polymer 1995;36(20):3849.
[44] Scott CE, Macosko CW. Polym Eng Sci 1995;35(24).
[45] Scott CE, Macosko CW. Polymer 1994;35(25).
[46] Fowler MW, Baker WE. Polym Engng Sci 1988;28(21):1427.
[47] Product literature, Perstorp Polyols Boltorn Material Data Brochure, 1998.

[48] Product literature, Dylark Engineering Resins. ARCO Chemical Co., 1990.
[49] Product literature, General Polymers Materials Data Sheet. Ashland Chemical Co., 1997.
[50] Beck Tan NC, Tai SK, Briber M. Polymer 1996;37(16):3509.
[51] Chang F, Hwu Y. Polym Eng Sci 1991;31(21):1509.
[52] Brannock GR, Barlow JW, Paul DR. J Polym Sci 1991;29:413.
[53] Simmons A, Baker WE. Polym Commun 1990;31:20.
[54] Brown SB. Annu Rev Mater Sci 1991;21:463–89.
[55] Mulkern TJ. MS thesis, University of Massachusetts Lowell, PL-28, 1998.
[56] Goodrich JE, Porter RS. Polym Eng Sci. January 1967.
[57] Bucknall CB. Toughened plastics, London: Applied Science Publishers, 1977.
[58] Willis JM, Favis BD. Polym Eng Sci 1990;30(17):1073.
[59] Folkes MJ, Hope PS. Polymer blends and alloys, New York: Van Nostrand Reinhold, 1993.
[60] Majumdar B, Paul DR, Oshinski AJ. Polymer 1997;38(8):1787–808.
[61] Forteln I, Zivn A. Polymer 1998;39(12):2669–75.
[62] Schoolenberg GE, During F. Polymer 1998;39(4):757–63.
[63] Taylor GI. Proc R Soc Lond A 1934;146:501.
[64] Wu S. Polym Engng Sci 1987;27:335.
[65] Utracki LA, Shi ZH. Polym Engng Sci 1992;32:1824.
[66] Peterson B. Technical data brochure, Perstorp, Sweden, January 1996.
[67] Paul DR. Polymer blends, New York: Academic Press, 1978.
[68] Paul DR. Encyclopedia of polymer science and engineering, 12. New York: Wiley, 1986 p. 399.
[69] Paul DR. Polymer blends, New York: Academic Press, 1978.
[70] Sperling LH. Introduction to physical polymer science, New York: Wiley, 1992.